Vehicle Localisation using Asphalt Embedded Magnetometer Sensors

1st Giammarco Valenti
Dept. of industrial Engineering
University of Trento
Trento, Italy
giammarco.valenti@unitn.it

2nd Francesco Biral
Dept. of industrial Engineering
University of Trento
Trento, Italy
francesco.biral@unitn.it

3rd Daniele Fontanelli
Dept. of industrial Engineering
University of Trento
Trento, Italy
daniele.fontanelli@unitn.it

***Abstract*—While advanced driving assistance systems for vehicles are becoming mature in urban and freeway scenarios, the enabling service of precise localisation with respect to the road lane is gaining more and more attention in the last decade. Indeed, having knowledge of the precise location of the vehicle allows safer and more efficient solutions, especially when those information are shared among multiple vehicles. This manuscript deals with the definition of an effective and simple nonlinear least squares solution for estimation and tracking of vehicles using multiple magnetometers embedded on the lateral road stripes. The solution relies on a classical model of magnetometer measurements and it is made robust by adding turning the classic least square solution to a constrained optimisation problem dictated by known road quantities (i.e., curvature and lanes dimensions). A first set of results sound promising for an effective application of the proposed algorithm to vehicle tracking.**

***Keywords*—Vehicle localisation, Magnetometers, Weighted Least Squares estimation**

I. Introduction

Precise vehicle localisation in the road lanes is a task of paramount importance for the deployment of intelligent vehicles equipped with Advanced Driving Assistance Systems (ADAS) or Autonomous Driving (AD) capabilities [1]. The most widespread solution adopted for precise localisation is the data fusion of on board sensors (with various combinations) and the use of high resolution road maps. Vehicles equipped with a rich set of sensors can precisely localise themselves at lane level but with a quite expensive equipment. Additionally, they cannot solve alone the problem of identifying object not in line of sight or occluded by other vehicles or infrastructure/urban elements (e.g. buildings). A solution to extend the electronic horizon of intelligent vehicles is provided by Vehicle-to-Vehicle and Vehicle-to-infrastructure communications (jointly referred as V2X communication) [2]. In particular, the road equipped with sensors in specific locations, such as intersections, may detect the presence of vehicles and vulnerable road users and broadcast the information for the benefit of all intelligent vehicles in the area. The V2X approach is also low cost and is more suitable to powered two wheelers.

The work presented in this manuscript is partially sponsored by SAFE STRIP (Safe and green sensor technologies for self-explaining and forgiving road interactive applications) project which has received funding from the European Research Council (ERC) under the European Union's Horizon 2020 research and innovation programme (Grant Agreement n° 723211).

Among the sensors used for the infrastructure, videocameras are emerging as the most effective, especially when combined with the advancement of deep neural networks, but their efficacy is jeopardised by low visibility in bad weather conditions (e.g. heavy rain, fog, etc.) or occlusions in complex urban environments. The SAFE STRIP EU project [3] has proposed to support intelligent transport systems (ITS) by designing and developing road strips that embed various sensors to provide a large set of static passive info (i.e. speed limit, asphalt characteristics, road geometry and layout) and dynamic environmental/road parameters (e.g. temperature, humidity, ice, ambient light, water). For the vehicle detection at lane level, switches embedded in the strip placed transversally to the road direction were used. The adopted solution provides in-lane position and vehicle speed, but can hardly support vehicle tracking and accurate in-lane orientation. To overcame this problem, we propose to use magnetometers embedded in the strips placed along the road direction. This solution has the advantage to be more robust (i.e. strips are not continuously pressed by vehicles), can work in any conditions and it is suitable to track the vehicle position and other quantities (e.g. vehicle sideslip estimation fusing magnetometers and GPS data [4], [5]) for longer stretch of the road. The use of magnetometers mounted on road surface is not new, however they are manly employed to classify [6] and/or detect the vehicles and estimate their speeds [7] for traffic management applications [8]. In [9], a bank of Extended Kalman Filters is proposed for tracking road vehicles that are travelling in the vicinity of two magnetometers place on the two side of the roads. Authors in [10] propose to fuse road-mounted accelerometer and magnetometer measurements for vehicle tracking and traffic monitoring using a multirate particle filters. The scenario investigated considers a single couple of two sensors and a vehicle moving in straight line on a straight road. In [11] and array of 4 magnetometers is used to measure the magnetic field of a moving target but the tracking problem is not the focus of the work. Finally a progressive extended Kalman filter is proposed to track a magnetic dipole [12]. The algorithm is tested on an intersection using two magnetometers placed on the road side.

The solution that we propose here is meant to be completely independent from vehicle on-board sensors and it aims at tracking vehicles along curvy roads with lane level accuracy including vehicle orientation in the lane. The estimated information are ment to be shared with intelligent vehicles and road operators to support cooperative safety

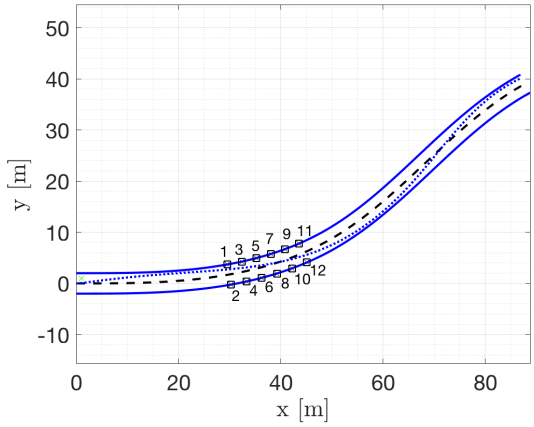

Fig. 1. Road and magnetometers deployment, denoted with a unique identified and a square marker in the figure. The actual vehicle trajectory is also reported with a dotted line.

functions via V2X communication of new 5G solutions.

The paper is organised as follows. In Section II, we set up the problem introducing the models adopted and the manuscript notation. The solution is detailed in Section III, while a preliminary simulative validation is reported and discussed in Section IV. Finally, in Section V, we present our conclusions and announce future work directions.

II. Background Material and Problem Formulation

The problem we are addressing in this paper is the localisation of a vehicle on a road using magnetometers placed on the side of the road in known positions, as represented in Figure 1 with squares on the road sides. The vehicle model adopted in this paper corresponds to the kinematics of a point mass vehicle described in curvilinear coordinates (i.e. road coordinates). It is briefly described here in its discretised version, adopting a sampling time of T_s

$$\begin{aligned} u_{k+1} &= u_k, \\ s_{k+1} &= s_k + T_s u_k, \\ n_{k+1} &= n_k + T_s \xi_k u_k, \\ z_{k+1} &= z_k, \\ \xi_{k+1} &= \xi_k - T_s \kappa(s_k) u_k, \end{aligned} \tag{1}$$

where we adopted the notation $u_k = u(kT_s)$, as customary. u_k is the forward velocity of the vehicle, supposed to be time-invariant in the short road section where the magnetometers are placed, s_k is the curvilinear abscissa of the vehicle defined by the road centre line, n_k is the normal displacement with respect to that line and z_k is the height of the vehicle with respect to the road plane (constant as well). Finally, ξ_k is the relative orientation of the vehicle with respect to the tangent of the road and $\kappa(s_k)$ is the curvature of the vehicle trajectory in the location s_k, which is supposed to be compensated by the yaw rate. Obviously, all these quantities are referred to time kT_s. We generically refer to the vehicle state as the vector $\mathbf{p}_k = [s_k, n_k, z_k, \xi_k]^T$.

A. Sensors model

The magnetometer model here adopted is the one presented in [9] and here detailed after the following simplifying assumptions.

Assumption 1: The magnetometer is aligned with the road, i.e. its x axis is tangent to the road.

Assumption 2: The curvature of the road with respect to the magnetometer range is negligible.

Notice that Assumption 1 can be easily verified by calibration of the deployed sensor, while Assumption 2 is easily verified in the majority of the common roads. In practice, this constraint may simply impose a limit on the sensor deployment road sectors, but it proves to be very relevant. In fact, given the i-th magnetometer position in road coordinates be $\mathbf{p}_{i,m} = [s_{i,m}, n_{i,m}, z_{i,m}]^T$ with $z_{i,m} = 0$, $\forall i$, it is possible to write the cartesian coordinates of the vehicle in the magnetometer reference frame as

$$\begin{aligned} x_{i,k} &= s_{i,k} - s_{i,m}, \\ y_{i,k} &= n_{i,k} - n_{i,m}, \end{aligned} \tag{2}$$

with the additional value of z_k in (1), which are denoted as $\mathbf{r}_{i,k} = [x_{i,k}, y_{i,k}, z_k]^T$.

Let $\mathbf{m}_0 = [m_{x_0}, m_{y_0}, m_{z_0}]^T$ be the magnetic dipole expressed in the vehicle reference frame, the overall magnetic dipole moment at time kT_s is given by [9]

$$\mathbf{m}_k = \mathrm{Rot}(\xi_k)\mathbf{m}_0 + \frac{d}{\mu_0}\mathbf{B}_0, \tag{3}$$

where $\mathrm{Rot}(\xi_k)$ is the rotation induced by the vehicle orientation ξ_k in (1), d is the target characteristic scalar factor, μ_0 is the scaling magnetic constant and $\mathbf{B}_0$ is the constant dipole bias induced by the earth magnetic field, which is supposed to be known (if not, it can be estimated with the magnetometers in static conditions, i.e., when no vehicles are detected).

Therefore, the i-th magnetometer measurements can be expressed as

$$\begin{aligned} &\mathbf{z}_{i,k} = h_i(\mathbf{r}_{i,k}, \mathbf{m}_k, \mathbf{B}_0) + \boldsymbol{\varepsilon}_{i,k} = \\ &= \mathbf{B}_0 + \frac{\mu_0}{4\pi\|\mathbf{r}_{i,k}\|^5}\left(3\mathbf{r}_{i,k}\mathbf{r}_{i,k}^T - \|\mathbf{r}_{i,k}\|^2 I_3\right)\mathbf{m}_k + \boldsymbol{\varepsilon}_{i,k} = \\ &= \mathbf{B}_0 + H_{i,k}\mathbf{m}_k + \boldsymbol{\varepsilon}_{i,k} \approx \\ &\approx \mathbf{B}_0 + H_{i,k}\mathrm{Rot}(\xi_k)\mathbf{m}_0 + \frac{d}{\mu_0}\mathbf{B}_0 + \boldsymbol{\varepsilon}_{i,k}, \end{aligned} \tag{4}$$

where I_3 is the identity matrix of dimension 3×3 and $\boldsymbol{\varepsilon}_k$ are the measurements uncertainty, supposed to be zero-mean, white, Gaussian with covariance matrix R. Notice that in (4) we made the simplifying assumption that the second term in the right-hand side of (3) is approximately constant, so has to estimate separately the contribution of d.

B. Problem formulation

The objective of this paper is to design an estimator that is able to track the vehicle position in road coordinates $\mathbf{p}_k$ described by the dynamic model (1), to estimate the vehicle dipole $\mathbf{m}_0$ and to estimate the unknown target scalar factor d using the noisy measurements (4) coming from $m \geq 1$ magnetometers placed on the road side(s) (a possible

deployment with $m = 12$ is reported in Figure 1). In this manuscript, we assume that the velocity of the vehicle u_k is not part of the estimation process and it is assumed given (e.g., the vehicle can transmit this information when it travels nearby the magnetometers). Notice that this assumption can be easily verified assuming the vehicle is endowed with a simple wireless connection (e.g., V2X [13] or ITS-G5 [14] communication). Notice additionally that estimating the position $\mathbf{p}_k$ in road coordinates from just a single magnetometer (i.e. $m \geq 1$) allows to easily fuse together the measurements from multiple magnetometers as well as to set up distributed estimation processes. In this first version of the paper, we consider communication between the magnetometer to propagate suitable initial estimation conditions for the nonlinear regressors, as it will be explained in the next sections.

III. A Nonlinear Least Squares Solution

The solution we are presenting in this manuscript considers both the highly nonlinear measurement function (4) and the system dynamics in (1), whose longitudinal velocity u_k is supposed to be unknown and constant. The very first step to design an estimator is to verify if the state of interest $\mathbf{a}_k = [\mathbf{p}_k^T, \mathbf{m}_0^T, d]^T$ is actually observable. To this end, we rely on the results in [9], where it is stated that the problem is observable even for a single magnetometer (i.e. $m = 1$) if some priors are known on the vehicle road position and the vehicle is not moving radially with respect to the magnetometer, which is not the case at hand due to Assumptions 1 and Assumption 2.

In what follows we present the proposed approach. We first present how the single magnetometer problem can be solved and then we propose our strategy when $m > 1$ in the road sector.

A. State estimation with $m = 1$

Let us suppose that at time kT_s a number of k consecutive measurements are collected by the only i-ht magnetometer available with a sampling time of T_s. We first set-up the following simple vehicle detection algorithm: if there exists

$$\left\| \mathbf{z}_{i,k} - \frac{\sum_{j=1}^{k-1} \mathbf{z}_{i,j}}{k-1} \right\| > \Delta_z,$$

where Δ_z is a tuning threshold that depends on the available hardware and on the covariance matrix R of the uncertainties in (4), a vehicle is detected at time $k = \underline{k}$. Hence, from $k \geq \underline{k}$ all the measurements can be used to track the vehicle, until for some $\overline{k} > \underline{k}$ the following holds

$$\left\| \mathbf{z}_{i,\overline{k}} - \frac{\sum_{j=1}^{\underline{k}-1} \mathbf{z}_{i,j}}{\underline{k}-1} \right\| < \Delta_z.$$

From the previous algorithm it follows that $\forall k \in [\underline{k}, \overline{k}]$ the magnetometer returns a valid measurement of a vehicle to be adopted in the estimation of $\mathbf{a}_k$.

The valid set $[\underline{k}, \overline{k}]$ is split into chunks of l consecutive measurements. In practice, at time $(\underline{k}+l-1)T_s$, it is possible to derive the first estimate. By denoting with $k^\star = \underline{k}$, the objective of the estimator is then to make use of the measurements $\mathbf{z}_{i,k^\star}, \ldots, \mathbf{z}_{i,k^\star+l-1}$ to retrieve an estimate $\hat{\mathbf{a}}_{k^\star}$ (we use the notation $\hat{\cdot}$ to denote estimated quantities), which is detailed in Section III-B. Once $\hat{\mathbf{a}}_{k^\star}$ is available, the same idea of [15] can be applied and, hence, we can propagate such estimate to time $\hat{\mathbf{a}}_{k^\star+l-1}$. Recalling that $\hat{\mathbf{a}}_{k^\star} = [\hat{\mathbf{p}}_{k^\star}^T, \hat{\mathbf{m}}_0^T, \hat{d}]^T$, only $\hat{\mathbf{p}}_{k^\star}$ is time varying and so it is the only quantity to be propagated. To this end, we can write the closed form propagation derived from (1) and reported next

$$\begin{aligned}
s_{k^\star+l-1} &= s_{k^\star} + T_s \sum_{j=0}^{k^\star+l-2} u_{k^\star+j}, \\
n_{k^\star+l-1} &= n_{k^\star} + T_s \xi_{k^\star} \sum_{j=0}^{k^\star+l-2} u_{k^\star+j} + \\
&\quad - T_s^2 \sum_{j=0}^{k^\star+l-2} u_{k^\star+j} \sum_{q=0}^{j-1} \kappa(s_{k^\star+q}) u_{k^\star+q}, \\
z_{k^\star+l-1} &= z_{k^\star}, \\
\xi_{k^\star+l-1} &= \xi_{k^\star} - T_s \sum_{j=0}^{k^\star+l-2} \kappa(s_{k^\star+j}) u_{k^\star+j},
\end{aligned} \tag{5}$$

which can be computed using the yaw rate compensation.

The main advantage of the proposed approach relies on the fact that the estimator objective turns to be an unknown but constant value $\hat{\mathbf{a}}_{k^\star}$, thus opening to solutions of the Least Squares (LS) family (see Section III-B). Moreover, once $\hat{\mathbf{a}}_{k^\star+l-1}$ is derived, it is sufficient to set $k^\star = k^\star + l$ and then starts the iteration with the new set of l measurements.

B. Constrained nonlinear least squares

We now presents the details of the estimator that, using the measurements $\mathbf{z}_{i,k^\star}, \ldots, \mathbf{z}_{i,k^\star+l-1}$, computes the estimate $\hat{\mathbf{a}}_{k^\star}$. To this end, we first recall that the measurement function in (4) can be equivalently rewritten as

$$h_i(\mathbf{r}_{i,k}, \mathbf{m}_k, \mathbf{B}_0) = h_i(\mathbf{a}_k, \mathbf{B}_0),$$

which allows to write the nonlinear LS solution

$$\hat{\mathbf{a}}_{k^\star} = \arg\min_{\mathbf{a}_{k^\star}} \sum_{j=0}^{l-1} \delta \mathbf{z}_{i,k^\star+j}^T \delta \mathbf{z}_{i,k^\star+j}, \tag{6}$$

where $\delta \mathbf{z}_{i,k^\star+j} = \mathbf{z}_{i,k^\star+j} - h_i(\mathbf{a}_{k^\star+j}, \mathbf{B}_0)$. We first notice that by means of (5), all the elements in $\mathbf{a}_{k^\star+j}$, $\forall j > 0$, can be expressed in terms of $\mathbf{a}_{k^\star}$, thus making the proposed solution well grounded. Moreover, this problem turns to be solvable with a minimum of $l = 3$ consecutive measurements from the single magnetometer (i.e., 3 equations per measurements, which makes a total of $3l = 9$ equations in 8 unknowns in $\mathbf{a}_{k^\star}$).

To solve the nonlinear problem in (6), we adopted the Gauss-Newton method. Since this is a purely numerical method, we impose the minimum value of the update vector to continue for the search of the minimum to be $\Delta_{\mathbf{a}_{k^\star}} > \underline{\Delta}_{\mathbf{a}_{k^\star}}$, while otherwise the method stops and return the last computed $\hat{\mathbf{a}}_{k^\star}$. However, due to the highly nonlinear characteristics of the problem, we impose two constraints, thus turning the problem to an optimal constrained problem. First, we notice that the gradient-descent like approach of Gauss-Newton should be limited. Therefore, whenever an update vector $\Delta_{\mathbf{a}_{k^\star}}$

is computed with Gauss-Newton method, we impose the following check:

$$\Delta_{\mathbf{a}_{k^\star}} = \begin{cases} \overline{\Delta}_{\mathbf{a}_{k^\star}} \frac{\Delta_{\mathbf{a}_{k^\star}}}{\|\Delta_{\mathbf{a}_{k^\star}}\|}, & \text{if } \|\Delta_{\mathbf{a}_{k^\star}}\| > \overline{\Delta}_{\mathbf{a}_{k^\star}}, \\ \Delta_{\mathbf{a}_{k^\star}}, & \text{otherwise.} \end{cases}$$

This way, the algorithm moves with a slower pace towards the solution, but it is more robust to numerical errors in the computation of the Gauss-Newton step. Of course, both $\underline{\Delta}_{\mathbf{a}_{k^\star}}$ and $\overline{\Delta}_{\mathbf{a}_{k^\star}}$ need to be fine tuned with respect to the assumed noise level in the magnetometer.

The second constraint is on the feasible values that the vector $\hat{\mathbf{a}}_{k^\star}$ may assume. In particular, it is easy to see that $\hat{\mathbf{p}}_{k^\star}$ are easily limited by the road dimension and by the fact that the vehicle is not performing a U-turn in front of the magnetometers, thus imposing $\hat{\xi}_{k^\star} \in [-\pi/2, \pi/2]$ rad. It is also assumed a maximum value for the magnetic dipole $\hat{\mathbf{m}}_k$ and a maximum and minimum value for $\hat{d}$. To respect the imposed constraints, we adopt the constrained projector reported in [16], which returns the solution that respect the constraints and it is the closest (with respect to the Euclidean norm) to the computed Gauss-Newton solution.

C. State estimator with $m > 1$

The extension to multiple magnetometers increases the robustness and the effectiveness of the method. For this first version of the paper, each magnetometer carries out its own estimation based on its own l measurements and the algorithm presented in Section III-B. The connection among the different magnetometers is offered by the iterative nature of the nonlinear LS. Indeed, it is easy to notice that once the i-th magnetometer has computed the estimates $\hat{\mathbf{a}}_{k^\star}$ using the measurements at time $k^\star T_s$ to $(k^\star + l - 1)T_s$, it should use the next available measurements from time $(k^\star + l)T_s$ to $(k^\star + 2l - 1)T_s$ to determine the estimate $\hat{\mathbf{a}}_{k^\star+l}$. However, this second estimate does not start from a generic point in the feasible domain, but its first guess is just given by $\hat{\mathbf{a}}^g_{k^\star+l}$, i.e. by $\hat{\mathbf{a}}_{k^\star}$ propagated forward using (5). This way, after the first solution is retrieved, the next iteration of the algorithm will be far less critical and certainly faster.

This propagation approach adopted for the single magnetometer, can be applied as well to propagate the estimates among the different magnetometers. Let us suppose that that a first estimate $\hat{\mathbf{a}}_{k^\star}$ is retrieved for the i-th magnetometer. It is then possible to revert (2) to have an estimate in global road coordinates for $\hat{\mathbf{p}}_{k^\star}$, while, of course, the other two components of $\hat{\mathbf{a}}_{k^\star}$, i.e., $\hat{\mathbf{m}}_0$ and $\hat{d}$ are not time varying nor depending on the chosen reference frame. Using again (2) with respect to the j-th magnetometer position, is then possible to have a good initial condition for the j-th magnetometer and measurements $\mathbf{z}_{j,k^\star}, \ldots, \mathbf{z}_{j,k^\star+l-1}$ as well, thus improving performance and robustness of the estimation procedure.

IV. Simulation Results

In this section, we present the first simulation results for the algorithm presented in Section III. We assume a sampling time of $T_s = 50$ ms for each magnetometer and a number of $m = 12$ sensors, deployed as depicted in Figure 1. The

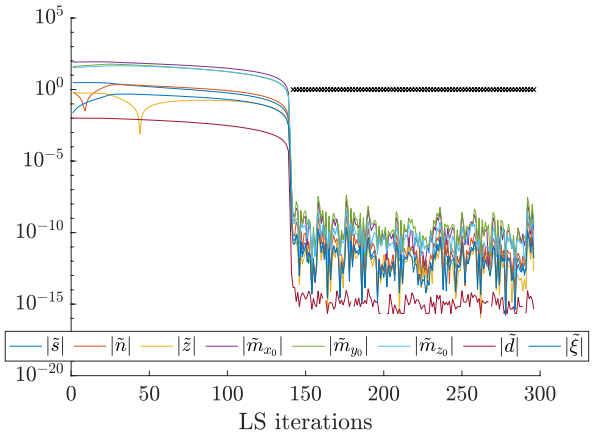

Fig. 2. Nonlinear LS estimation errors as a function on the number of steps of the algorithm. The end of each computation is signed with a black cross.

value of the scaling magnetic constant is imposed to be $\mu_0 = 4\pi \cdot 10^{-7}$, while the terrestrial constant magnetic field is $\mathbf{B}_0 = [13.5, 13.5, 1.6]^T$. We assume that the actual value of the dipole is $\mathbf{m}_0 = [100, 100, 100]^T$ Tesla, instead the vehicles is supposed to move along the dotted trajectory in Figure 1. The covariance matrix of the Gaussian uncertainties in (4) is $R = \sigma_\varepsilon^2 I_m$ (i.e., the uncertainties $\boldsymbol{\varepsilon}_k$ are white and uncorrelated along the different magnetometer sensed quantities), with $\sigma_\varepsilon = 0.01$ Tesla.

For the proposed estimation algorithm, the threshold for data valid detection in Section III-A is set to $\Delta_z = 0.05$ Tesla, while the minimum number of measurements to estimate $\hat{\mathbf{a}}_k$ described in Section III-B is $l = 3$. Moreover, the tolerance for the Gauss-Newton method are $\underline{\Delta}_{\mathbf{a}k^\star} = 10^{-3}$ and $\overline{\Delta}_{\mathbf{a}k^\star} = 1$. Due to the road characteristics and to impose the constraints in Section III-B, we assume that a valid estimate in the magnetometer relative system (2) is when $\hat{x}_{i,k} \in [-8, 8]$ m, $\hat{y}_{i,k} \in [-4, 4]$ m, $\hat{z}_{i,k} \in [0.1, 1]$ m, $\hat{\xi}_{k^\star} \in [-\pi/2, \pi/2]$ rad. Moreover, the maximum value for the magnetic dipole $\hat{\mathbf{m}}_k$ along the different components is between 0 and 200 Tesla. Finally, the target characteristic scalar factor estimate $\hat{d} \in [0.5, 2]$.

Figure 2 reports the absolute value of the estimation error $\tilde{\mathbf{a}}_k = \mathbf{a}_k - \hat{\mathbf{a}}_k$ as a function of the nonlinear LS iteration steps. We first notice that the first estimate is obtained after around 140 steps (i.e., the first cross black cross position location in Figure 2), since the initial condition is simply computed by generating random initial conditions verifying the constraints previously mentioned. However, after the first estimate, the algorithm speeds up and generate an estimate right after one step (hence, the sequence of black crosses appears to be a solid think line in Figure 2).

Notice that the estimation error is considerably small, which testify that the approach validated with these preliminary results sounds promising. As a further proof, we report also the absolute value of the estimation error as a function of the vehicle trajectory (see Figure 3): between $k = 47$ and $k = 87$ time steps, the vehicle is located in the road section equipped with the sensors depicted in Figure 1 and, hence, tracked.

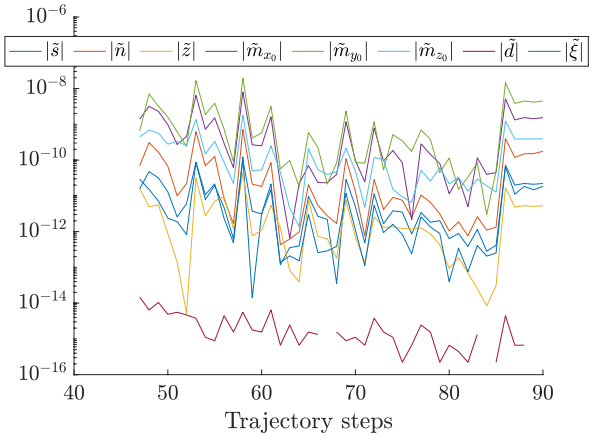

Fig. 3. Absolute errors in terms of vehicle trajectory.

We are now presenting the results considering an increasing noise on the vehicle velocity (assumed to be zero mean, white, normally distributed and with standard deviation $\sigma_u \in \{0, 0.001, 0.01, 0.1\}$ m/s) and a variable number of measurements to estimate $\hat{\mathbf{a}}_k$ ranging between $l \in \{3, \ldots, 10\}$. For space limits, we report the mean, maximum and minimum absolute error only for the quantities n and m_{x_0} in Figure 4-a and Figure 5-a, respectively, being all the others comparable and with similar behaviours. It is easy to see how the uncertainty on the forward velocity plays a major role in the achievable estimation uncertainty, which can be, however, mitigated by increasing the number of measurements. In order to test the proposed solution in non-nominal conditions, Figure 4-b and Figure 5-b show the estimation error of the same quantities n and m_{x_0} when z_k, i.e. the hight of the vehicle w.r.t. the road plane, is variable. In particular, we have assumed z_k varying with a sinusoidal function ranging between 0 and 0.8. Notice that the lower value is outside the admissible range for z_k previously hypothesised. It is clearly visible from Figure 4-b and Figure 5-b that such variability is predominant in the estimator performance, nonetheless the performance remains acceptable with any value of uncertainty or number of measurements.

Finally, Figure 6 reports the mean execution time of the algorithm in all the cases of Figure 4 and Figure 5. It is clearly visible how the computational burden, here evaluated on a laptop endowed with an Intel Core i9 at 2.9 GHz but considering a non optimised code written in Matlab, is well within the sampling time $T_s = 50$ ms of the sensors, and can accommodate the communication phase with the vehicle and easily executable on an embedded platform.

V. Conclusion

We proposed an effective and simple nonlinear LS solution for estimation and tracking of vehicles using multiple magnetometers. The solution relies on a classical model of the measurements and it is made more robust by adding constraints on the estimated quantities. A first set of results sound promising for an effective application of the algorithm to this specific problem. In the future works, we are planning to relax the constraints on the vehicle curvature knowledge, to fuse the sensors readings together in the estimator and

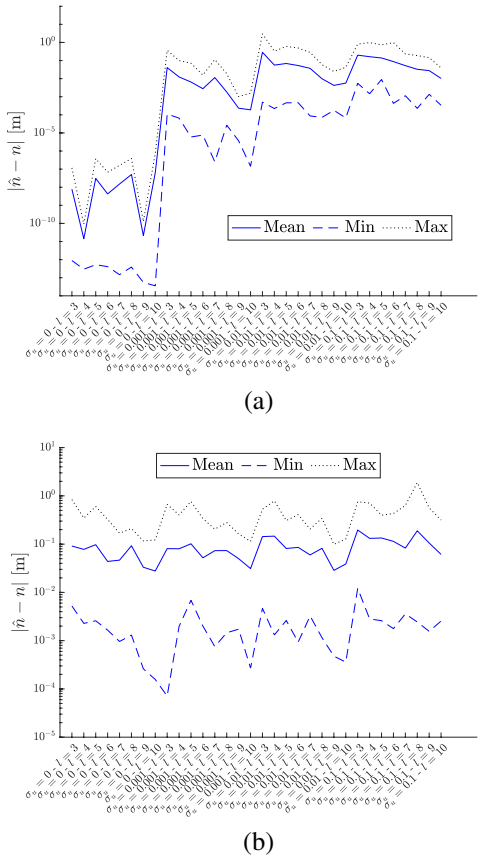

Fig. 4. Absolute errors in terms of forward velocity uncertainty σ_u and consecutive measurements considered l for the quantity n with (a) constant and (b) varying z_k.

to improve the estimator performance by considering the covariance matrix of correlated uncertainties (i.e., nonlinear Weighted LS solution). Furthermore, future developments will focus on the determination of conditions for the detection of multiple vehicles as well as on the simultaneous estimation of the vehicle(s) longitudinal velocity. We will also study how to remove the yaw rate compensation assumption and compare the proposed Gauss-Newton solution to the Levenberg-Marquardt approach. Finally, experimental investigation of the effectiveness of the solution in a real test case scenario is planned. In particular, we are planning to work in collaboration with CRF-Trento and use centimetre level GPS-RTK ground truth reference for the tracked vehicle.

References

[1] S. Kuutti, S. Fallah, K. Katsaros, M. Dianati, F. Mccullough, and A. Mouzakitis, "A survey of the state-of-the-art localization techniques and their potentials for autonomous vehicle applications," *IEEE Internet of Things Journal*, vol. 5, no. 2, pp. 829–846, 2018.

[2] M. N. Ahangar, Q. Z. Ahmed, F. A. Khan, and M. Hafeez, "A survey of autonomous vehicles: Enabling communication technologies and challenges," *Sensors*, vol. 21, no. 3, 2021. [Online]. Available: https://www.mdpi.com/1424-8220/21/3/706

[3] F. Biral, G. Valenti, E. Bertolazzi, and A. Steccanella, "Cooperative safety applications for c-its equipped and non-equipped vehicles supported by an extended local dynamic map built on safe strip technology," in *2019 15th International Conference on Distributed Computing in Sensor Systems (DCOSS)*, 2019, pp. 733–740.

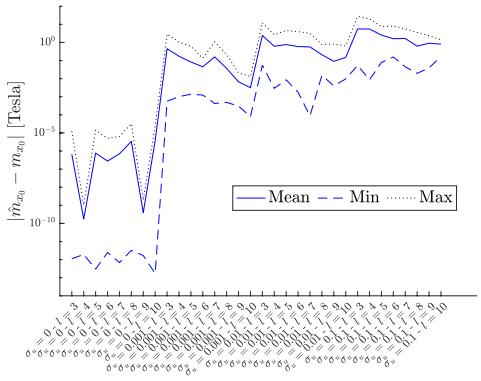

(a)

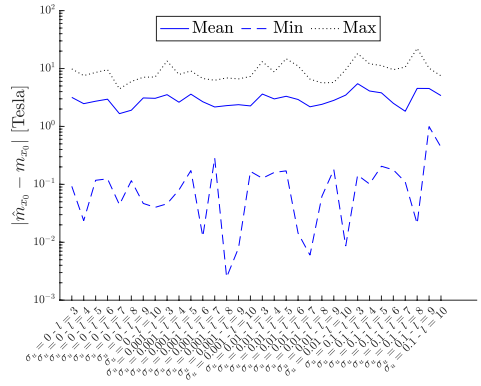

(b)

Fig. 5. Absolute errors in terms of forward velocity uncertainty σ_u and consecutive measurements considered l for the quantity m_{x_0} with (a) constant and (b) varying z_k.

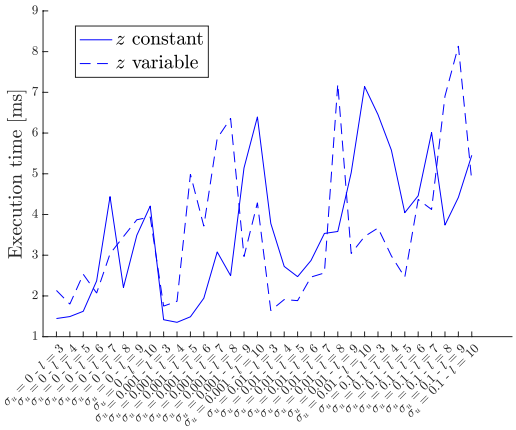

Fig. 6. Algorithm average execution times in all the cases of Figure 4 and Figure 5.

[4] J. Yoon and H. Peng, "Robust Vehicle Sideslip Angle Estimation Through a Disturbance Rejection Filter That Integrates a Magnetometer With GPS," *IEEE Transactions on Intelligent Transportation Systems*, vol. 15, no. 1, pp. 191–204, 2014.

[5] J.-H. Yoon, S. E. Li, and C. Ahn, "Estimation of vehicle sideslip angle and tire-road friction coefficient based on magnetometer with gps," *International journal of automotive technology*, vol. 17, no. 3, pp. 427–435, 2016.

[6] R. A. Kerekes, T. P. Karnowski, M. Kuhn, M. R. Moore, B. Stinson, R. Tokola, A. Anderson, and J. M. Vann, "Vehicle classification and identification using multi-modal sensing and signal learning," in *2017 IEEE 85th Vehicular Technology Conference (VTC Spring)*, 2017, pp. 1–5.

[7] Y. Feng, G. Mao, B. Cheng, C. Li, Y. Hui, Z. Xu, and J. Chen, "Magmonitor: Vehicle speed estimation and vehicle classification through a magnetic sensor," *IEEE Transactions on Intelligent Transportation Systems*, pp. 1–12, 2020.

[8] N. Wahlström, R. Hostettler, F. Gustafsson, and W. Birk, "Classification of driving direction in traffic surveillance using magnetometers," *IEEE Transactions on Intelligent Transportation Systems*, vol. 15, no. 4, 2014.

[9] N. Wahlström and F. Gustafsson, "Magnetometer modeling and validation for tracking metallic targets," *IEEE Transactions on Signal Processing*, vol. 62, no. 3, pp. 545–556, 2014.

[10] R. Hostettler and P. M. Djurić, "Vehicle Tracking Based on Fusion of Magnetometer and Accelerometer Sensor Measurements With Particle Filtering," *IEEE Transactions on Vehicular Technology*, vol. 64, no. 11, pp. 4917–4928, 2015.

[11] X. Zhang, X. Kang, X. Chen, H. Lv, Z. Geng, L. Fan, and C. Kang, "Measurement of far field magnetic moment vector of a moving ferromagnetic object," *IEEE Sensors Journal*, vol. 20, no. 18, pp. 10 903–10 912, 2020.

[12] S. Zhou, S. Shan, H. Zhang, and Z. Dai, "Progressive Kalman Filter and Its Application in Magnetic Target Tracking," in *2019 4th International Conference on Mechanical, Control and Computer Engineering (ICMCCE)*, 2019.

[13] L. Hobert, A. Festag, I. Llatser, L. Altomare, F. Visintainer, and A. Kovacs, "Enhancements of V2X communication in support of cooperative autonomous driving," *IEEE Communications Magazine*, vol. 53, no. 12, pp. 64–70, 2015.

[14] V. Mannoni, V. Berg, S. Sesia, and E. Perraud, "A Comparison of the V2X Communication Systems: ITS-G5 and C-V2X," in *2019 IEEE 89th Vehicular Technology Conference (VTC2019-Spring)*, 2019, pp. 1–5.

[15] D. Fontanelli, F. Shamsfakhr, D. Macii, and L. Palopoli, "An Uncertainty-driven and Observability-based State Estimator for Nonholonomic Robots," *IEEE Trans. on Instrumentation and Measurement*, 2021, available on line.

[16] D. Simon, "Kalman filtering with state constraints: a survey of linear and nonlinear algorithms," *IET Control Theory & Applications*, vol. 4, no. 8, pp. 1303–1318, 2010.